# *Analysis of the Impact of Changing Weather Phenomena on the Timing and Discharge of the Uncompahgre, San Miguel, and Animas Rivers, Colorado*

K.A. Kelkar, J.R. Giardino, J. Vitek, and G. Gamache

2017, pp. 209-217. https://doi.org/10.56577/FFC-68.209

*in:*

*The Geology of the Ouray-Silverton Area*, Karlstrom, Karl E.; Gonzales, David A.; Zimmerer, Matthew J.; Heizler, Matthew; Ulmer-Scholle, Dana S., New Mexico Geological Society 68 th Annual Fall Field Conference Guidebook, 219 p. https://doi.org/10.56577/FFC-68

*This page is intentionally left blank to maintain order of facing pages.*

New Mexico Geological Society Guidebook, 68th Field Conference, Geology of the Ouray-Silverton Area, 2017, p. 209-217.



# ANALYSIS OF THE IMPACT OF CHANGING WEATHER PHENOMENA ON THE TIMING AND DISCHARGE OF THE UNCOMPAHGRE, SAN MIGUEL, AND ANIMAS RIVERS, COLORADO

Kaytan A. Kelkar[1], John R. Giardino[1, 2], John Vitek[1, 2], and Garrett Gamache[3]

[1]High Alpine and Arctic Research Group (HAARP), Department of Geology and Geophysics, Texas A&M University, College Station, TX 77843, kaytank@tamu.edu;
[2]Water Management and Hydrological Science Graduate Program, Texas A&M University, College Station, TX 77843;
[3]Consultant, Santa Barbara, CA 93101.

Abstract—The limited availability of fresh water coupled with growing agricultural and urban demands in the western United States is forcing cities and towns to be heavily dependent on montane water resources for domestic supplies. Thus, predicting the impact of weather trends and variability on water resources is necessary to ensure that current and future demands for water can be met. Understanding the hydrologic response related to weather phenomena in montane regions, requires an answer to the question: Do weather phenomena reduce or shift the timing and volume of montane streamflow regimes? Time-series analysis and General-Least-Squares (GLS) regression were used to determine if a link exists between weather phenomena and the timing and volume of discharge for the Uncompahgre, San Miguel, and Animas Rivers in southwestern Colorado. Time-series analysis did not reveal significant ($\alpha = 0.05$) trends in the timing of streamflow for the three drainage basins. With GLS regression, at a level of 0.99 significance, the selected variables explained that 56% of the variance was associated with the onset date of the spring-pulse, 84% of the variance was associated with the timing of peak streamflow, and 82% of the variance was associated with the date at which elevated streamflow ends, or subsides. Our research illustrates the necessary foundation that can be used to determine site-specific changes in streamflow regimes to make critical water resource management decisions more accurate.

## INTRODUCTION

Water resources in montane areas are approaching excessive liability. The problem of reduced water resources is being accelerated by the decreasing volume of readily available freshwater and increasing population. This dependence has made montane river systems worldwide the subject of significant research focusing on vulnerability and variability associated with climate change (Nolin, 2012). Recent studies conducted by the Intergovernmental Panel on Climate Change (IPCC) suggest that some of the most crucial and already observable impacts of climate change are changes in seasonal stream-flow patterns attributed to earlier seasonal snowmelt and diminishing accumulation of annual snow fall (Bernstein, 2007; Nolin, 2012).

When considering the impact of weather on stream-flow, changes in the patterns of stream-flows have typically been attributed to earlier snowmelt and the reduction of snowpack (Tague and Grant, 2009; Viviroli et al., 2011). Although snow accumulation and melt are the primary hydrologic inputs from a montane stream-flow perspective, several other first-order controls affect the spatial variability of the hydrologic response to weather phenomena (Jasper 2004; Uhlenbrook et al., 2005; Tague et al., 2008; Tague and Grant, 2009; Viviroli et al., 2011).

Our research focuses on three watersheds in the San Juan Mountains, southwestern Colorado (Fig. 1) with primary research objectives of determining if the timing of streamflow regimes has indeed shifted, and if so, to what extent is it related to specific weather phenomena. By analyzing three separate watersheds, our research demonstrates the extent to which the effects of weather phenomena on streamflow are site-specific.

With human demand continuously exceeding supply, the Upper Colorado River Basin (UCRB), generates approximately 90% of the total flow of the Colorado River, which is the principal source of water and hydropower in the southwestern U.S. (Ficklin et al., 2013; McCabe and Wolock, 2007). Multiple studies (Ficklin et al., 2013; McCabe and Wolock, 2007; Timilsena et al., 2009) have shown that water availability in the UCRB could significantly decline as a result of changing weather patterns. Based on predictions from the General Circulation Model (GCM), a 3.5° to 5.6°C increase in surface temperature, median spring stream-flow is projected to decline by 36% by the end of the 21st century, for the UCRB (Ficklin et al., 2013). More importantly, summer stream-flows for the UCRB are projected to decline with median decreases of 46%. Further research shows that stream-flow in the UCRB is also highly sensitive to inter-annual and inter-decadal phenomena (Timilsena et al., 2009). Ficklin (2013) suggests that an increase in stream-flow occurs during El Nino and a decrease in stream-flow occurs during La Nina.

Some studies (Rangwala and Miller, 2010) show that the San Juan Mountains have experienced a net warming of 1°C between 1895 and 2005. Most of this warming occurred between 1990 and 2005. Any evident hydrologic impact in the San Juan Mountains may serve as a good indicator of what will occur further downstream; the San Juan Mountains con-


FIGURE 1. Location of Uncompahgre (HUC: 14020006), Animas (HUC: 14080104), and San Miguel (HUC: 14030003) River watersheds, located in the San Juan Mountains, Colorado.

tribute significantly to the annual flow of the Colorado and Rio Grande Rivers (Rangwala and Miller, 2010).

Although a significant amount of research addresses the UCRB as a whole, little research has focused on specific montane rivers and changes associated with them. No research has studied changes in stream-flow and weather phenomena for the Uncompahgre, San Miguel, and Animas rivers.

## STUDY AREA

The study area encompasses adjacent watersheds of the Uncompahgre, San Miguel, and Animas Rivers located in the San Juan Mountains of southwestern Colorado (Fig. 1).

These watersheds are most suitable for this study because they represent varying hydrologic, geologic and topographic conditions and have sufficient periods of record. Because of varying geographic orientations and topography of each watershed, variations in weather patterns impact streamflow regimes.

The three watersheds are semi-arid with a low relative humidity and primary sources of precipitation in the watershed are winter snowfall and late summer monsoonal thunderstorms (Toney and Anderson, 2006). Average temperatures range from -12°C in the winter to 27°C in the summer (Uncompahgre Watershed Partnership, 2013). Annual precipitation averages over 76 cm in the high mountains, with 350 cm of snow in Ouray each year (Uncompahgre Watershed Partnership, 2013). Average monthly snowpack is greatest in March and April. Approximately 40% of the Animas River watershed is above 2400 m, allowing snowpack to accumulate from late fall to early spring (Ray et al., 2008).

## UNCOMPAHGRE RIVER WATERSHED

The Uncompahgre River Watershed (Hydrologic Unit Code (HUC): 14020006) (38°N, 107°W) is located north of the Animas River Watershed. The Uncompahgre River Watershed drains about 2888 $km^2$ (Nydick et al., 2012), and the river flows to the north from its headwaters near Ouray joining the Gunnison River near Olathe. In total, the Uncompahgre River flows ~120 km over an elevation loss of ~ 2100 m, resulting in a relatively steep gradient.

## ANIMAS RIVER WATERSHED

The Animas River Watershed (HUC: 14080104) (37°N, 107°W) is located to the south of the Uncompahgre River Watershed. The Animas River flows south, draining 3515 $km^2$ from its headwaters north of Silverton and flows through Durango, CO to Aztec, NM. Elevations range from greater than 4300 m at the headwaters to less than 1830 m at the confluence with the San Juan River near Aztec, NM.

## SAN MIGUEL RIVER WATERSHED

The San Miguel River Watershed (HUC: 14030003) (37°N, 107°W), located to the west of Animas and Uncompahgre Watersheds, drains about 4050 $km^2$. The river begins above Telluride, at elevations above 4000 m, and flows about 145 km northwest, to its confluence with the Dolores River. The San Miguel River System is considered one of the few remaining intact river systems in the U.S. (Inyan, 2001). With the exception of the effects of acid mine drainage, little research has focused on the San Miguel Watershed (Inyan and Williams, 2001).

## METHODOLOGY

Time-series analysis was used to identify any significant trends in the timing of montane streamflow regimes for Uncompahgre River Watershed (URW), San Miguel River Watershed (SMRW), and Animas River Watershed (ARW). Thus, selected time periods for analysis were based on the longest consecutive period of available data. The URW was analyzed from 1937 to 2012, the SMRW was analyzed from 1943 to 2011 and the ARW was analyzed from 1914 to 2012.

Daily streamflow data for each watershed was obtained through USGS, Hydro-Climate Data Network (HCDN) (Slack and Landwehr, 1994). Daily-mean streamflow data for each of the three watersheds were used to model the annual flow regime (Table 1). Flow regimes were modeled using calendar years rather than water years because water years (October, 1 to September, 30) split the streamflow record such that it did not accurately represent fall precipitation.

Daily temperature and precipitation data were obtained through the National Oceanic and Atmospheric Administration (NOAA). NOAA weather stations were selected based on proximity to the three watersheds as well as length of record (Table 2). The weather data that we used were average monthly maximum and minimum temperatures, and average monthly precipitation for each month over the entire period of record.

Flow regimes extended from beginning peak to end of annual stream-flows. The beginning of annual streamflow represents the onset of the spring-pulse, which is defined as the date at which the variance of the daily streamflow increases significantly (Stewart et al., 2004). Spring-pulse onset was identified using a moving five-day streamflow variance method, which establishes the date at which the variance within any five-day-period exceeds a threshold of 5% of the annual maximum variance. The moving five-day streamflow variance method was also used to determine the end of annual streamflow. Our study defines the end of streamflow as the date at which the variance of the daily streamflow decreases significantly. In general, the moving variance method identifies the date, for each annual hydrograph, at which streamflow substantially increases and decreases, for the beginning and end of annual streamflow, respectively.

The moving variance method avoids bias created by using the standard percentile method (McCabe and Clark, 2005), which does not capture the desired information. The standard percentile method describes annual hydrographs by the date at which certain percentages (typically 25%, 50% and 75%) of total streamflow are achieved. This method is not suitable for our study because the percentages are inherently dependent on total streamflow. The moving variance method determines the timing of flows (beginning, peak and end) independently of each other. This is crucial when considering montane streamflow because the timing of the onset of the spring-pulse is primarily dependent on snowmelt and not on summer or fall precipitation.

Similar to other studies, (McCabe and Clark, 2005; Regonda et al., 2005; Stewart et al., 2004) we characterized the peak flow by the calendar date at which fifty percent of the annual flow volume was reached. Data processing were completed using R©, a statistical computing environment capable of processing large data sets (Team, 2005).

For each stream gauge, autocorrelation and partial autocorrelation functions were used to identify dependency within the data. Further analysis involved General-Least-Squares (GLS) regression methods to find relationships between weather phenomena and timing and volume of the stream-flow regimes. Average monthly maximum and minimum temperatures and average monthly precipitation were chosen as independent explanatory variables. A least-squares regression analysis was used to model each of the following response variables: the beginning, peak, and end of annual stream-flows (according to the previous definitions).

We did additional regression analysis to model correlations between the predictor variables and the total annual streamflow values. This analysis requires streamflow data to be logarithmically transformed prior to the development of the regression model to normalize the distribution.

## RESULTS

Time-series analysis was employed to identify significant trends in the timing of montane streamflow regimes for the Uncompahgre River Watershed (URW), San Miguel River

TABLE 1. Stream-gage locations for the analyzed river watersheds.

| Station Number | Station Name | Drainage Area (km²) | Latitude | Longitude | Data Duration | Source |
|---|---|---|---|---|---|---|
| 09147500 | Uncompahgre River at Colona | 1160 | 38.33 | -107.78 | 1937-2012 | USGS |
| 09361500 | Animas River at Durango | 1792 | 37.28 | -107.88 | 1914-2012 | USGS |
| 09172500 | San Miguel River near Placerville | 803 | 38.04 | -108.13 | 1942-2011 | USGS |

TABLE 2. Weather-station locations for the examined river watersheds.

| Station | Station ID | Latitude | Longitude | Data Duration | Elevation (m) |
|---|---|---|---|---|---|
| Ouray | GHCND:USC00056203 | 38.02 | -107.668 | 1937-2012 | 2389.6 |
| Silverton | GHCND:USC00057656 | 37.808 | -107.663 | 1914-2012 | 2830.1 |
| Telluride 4WNW | GHCND:USC00058204 | 37.949 | -107.873 | 1942-2011 | 2635.3 |

Watershed (SMRW), and Animas River Watershed (ARW). The URW was analyzed from 1937 to 2012, the SMRW was analyzed from 1943 to 2011 and the ARW was analyzed from 1914 to 2012.

The timing of flow regimes was characterized by the beginning, peak, and end of annual streamflows. The beginning of annual streamflow represents the spring-pulse onset, it is the date at which the variance of the daily streamflow increases significantly (Stewart et al., 2004). Similarly, our study defines the end of annual streamflow as the date at which the variance of the daily streamflow decreases significantly. Similar to other studies (McCabe and Clark, 2005; Regonda et al., 2005; Stewart et al., 2004), the peak is characterized by the calendar date where fifty percent of the annual flow volume is achieved.

Table 3 shows that no strong trends in the timing of streamflow were observed for the three selected locations. Luce and Holden (2009) explain that the lack of a trend is likely a result of the non-linear relationship between snow accumulation and timing of snowmelt. Substantial year-to-year variance is also largely responsible for the poor model fit and low coefficients of determination ($R^2$). Regardless of poor linear fits, the slope and relative nature of the trends provide valuable insight concerning shifting flow regimes. The time series analysis can be best understood in analyzing plots of dates of the beginning, the peak, and the end of annual streamflows for each individual location.

Of the three observed watersheds, the URW experienced the most change throughout the period of record (Fig. 2). For the URW, spring-pulse onset occurred approximately 15 days earlier in 2012 than it did in 1937. This negative trend in spring streamflow is in agreement with most research concerning snow-dominated streams. A positive trend was observed at fifty percent of annual flow volume and end of annual flow. For the URW, in general, the date at which fifty percent of the annual flow volume was achieved occurred approximately ten days later in 2012 than it did in 1937. Streamflow ended approximately 25 days later suggesting that streamflow may be extending longer into the year.

For the SMRW, less change was observed, but the pattern in trends was similar to that of URW (Fig. 3). For the SMRW, the onset of the spring-pulse and when fifty percent of total flow volume occurred was approximately ten days earlier in 2011 than in 1943. The end of streamflow, however, showed a positive trend, ending approximately 15 days later in the year.

The ARW observed the least amount of change in flow regime throughout the period of study (Fig. 4). A negative trend

TABLE 3. Time-series analysis results for the beginning, peak and end of annual streamflow for the URW, SMRW and ARW. Model fit is described by coefficient of determination ($R^2$).

| Model | Coefficient of Determination ($R^2$) | | |
|---|---|---|---|
| | URW | SMRW | ARW |
| Beginning | 0.21 | 0.26 | 0.19 |
| Peak | 0.52 | 0.49 | 0.46 |
| End | > 0.01 | > 0.01 | > 0.01 |

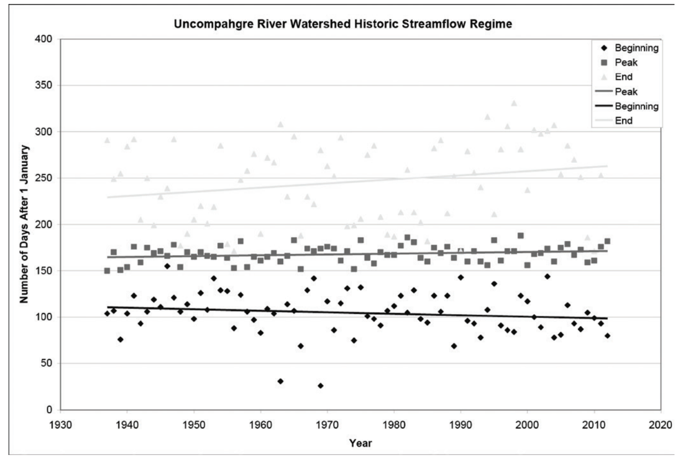


FIGURE 2. URW historic streamflow regime. URW time-series analysis for beginning, peak, and end of annual streamflow from 1937 to 2012.

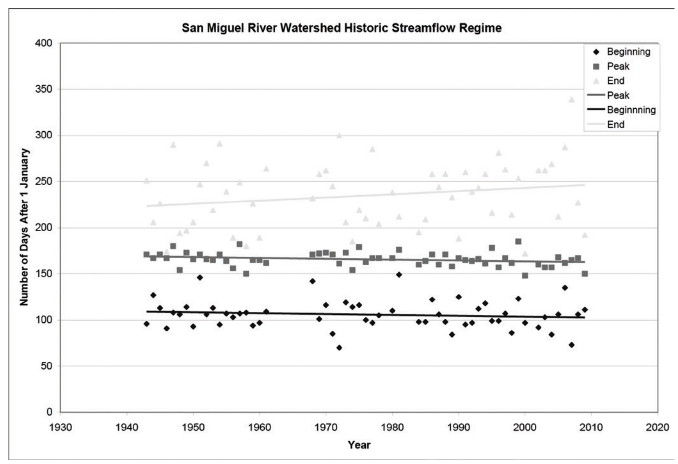


FIGURE 3. SMRW historic streamflow regime. SMRW time-series analysis for beginning, peak, and end of annual streamflow from 1943-2011.

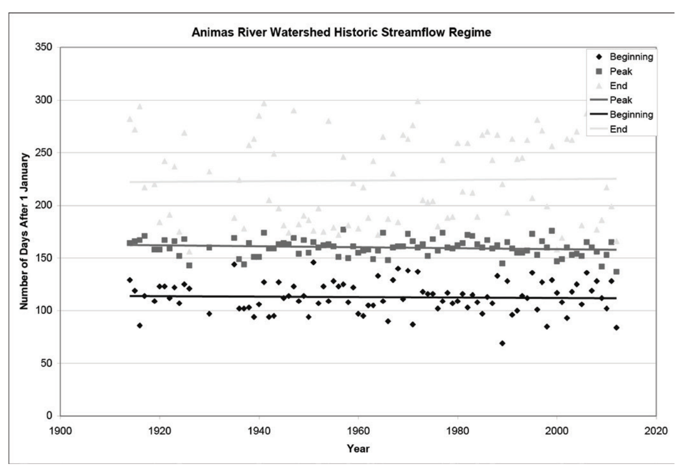


FIGURE 4. ARW historic streamflow regime. ARW time-series analysis for beginning, peak, and end of annual streamflow from 1914 to 2012.

was observed for the onset of the spring-pulse and the date when fifty percent of total flow volume occurred. Both events occurred approximately five days earlier in 2012 than in 1914. No substantial change occurred in the ending dates of annual streamflow.

Further analysis involved GLS regression to identify more explicit correlations between specific weather phenomena and the timing of montane stream-flow regimes. Average monthly maximum and minimum temperatures and average monthly precipitation were selected as independent explanatory variables, and the beginning, peak and end of annual streamflow were used as response variables. Study of the model determination coefficients in Table 4 shows that, in general, regression analysis is more suitable for modeling the timing of the peak and end of streamflow than the beginning.

GLS regression determined at a level of 0.99 significance, that the selected explanatory variables explained 56% of the variance associated with the date when the spring-pulse onset occurred (Fig. 5). For the beginning of annual streamflow model, the $R^2$ value was 0.56 and an adjusted $R^2$ was 0.35 (Table 4).

Table 5 shows that the most significant variables in determining the onset of the Spring-pulse are the average maximum February temperature, and average precipitation in April. These results suggest that on average, an increase of 1°C for the average maximum February temperature will result in the onset of the spring-pulse occurring approximately three days later, and an average precipitation increase of 0.1 mm for April typically results in the onset of the spring-pulse occurring approximately one day later. In general, increases in average maximum temperatures for winter months have the most substantial effect in terms of shifting the onset of the spring-pulse later and an increase in average minimum temperatures for spring months have the most substantial effect in terms of shifting the onset of the spring-pulse earlier. This impact is likely because an increase in average winter maximum temperatures prevents precipitation from falling as snow, resulting in less available snowpack come time for spring snowmelt. Conversely, an increase in average minimum temperatures for spring months results in earlier spring snowmelt.

When considering site-specific effects on the onset of spring-pulse, Table 6 shows that the San Miguel River Watershed was the only one that had a significant affect (α<0.95) on the timing of the onset of the spring-pulse. For the evaluated time period, the SMRW, on average, experienced the onset of the spring-pulse about 15 days earlier than the average for the three watersheds. This is likely the result of the SMRW having a larger percentage of lower elevation area.

Regarding the date when peak streamflow occurred, GLS regression determined at a level of 0.99 significance, that the selected explanatory variables explained 84% of the variance (Fig. 6). For the peak streamflow model, the $R^2$ was 0.84 and an adjusted $R^2$ was 0.68.

TABLE 4. GLS model results for the beginning, peak and end of streamflows for URW, SMRW and ARW. Model fit is described by coefficient of determination (R2).

| Model | Mean | Coefficients of Determination | |
|---|---|---|---|
| | | $R^2$ | Adj. $R^2$ |
| Beginning | 107 (17 April) | 0.56 | 0.35 |
| Peak | 165 (14 June) | 0.89 | 0.71 |
| End | 234 (22 Aug) | 0.82 | 0.31 |

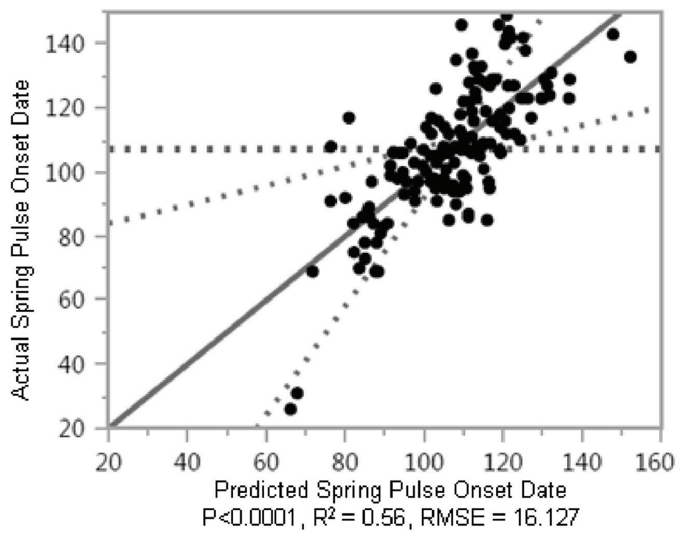


FIGURE 5. Spring-pulse onset model. GLS model fit for the date at which the average onset of the spring-pulse occurs (in number of days after 1 Jan), for all three watersheds. The mean of the response is demonstrated by the horizontal dotted-line, and the limits of the 0.90 confidence intervals are represented by the diagonal-dotted-lines.

TABLE 5. GLS beginning of streamflow model. Individual explanatory variable estimates (in days) with corresponding p-values, for all three watersheds (Levels of significance: * α = 0.05; ** α= 0.01).

| Month | Average Tmax. | | Average Tmin. | | Average Precipitation | |
|---|---|---|---|---|---|---|
| | Estimate | P- value | Estimate | P- value | Estimate | P- value |
| January | 1.67 | 0.32 | 1.32 | 0.33 | -0.15 | 0.60 |
| February | 2.82 | 0.04* | -1.37 | 0.29 | -0.13 | 0.55 |
| March | -1.64 | 0.27 | 1.92 | 0.17 | -0.22 | 0.22 |
| April | 0.32 | 0.85 | -2.32 | 0.25 | 0.73 | 0.001** |
| May | -0.29 | 0.85 | -3.33 | 0.14 | 0.22 | 0.44 |

TABLE 6. GLS beginning of streamflow mod)el site-specific estimates with corresponding p-values. Estimates in days, for all three watersheds (Levels of significance: * α = 0.05).

| Site | Estimate | P- value |
|---|---|---|
| URW | 16.83 | 0.10 |
| ARW | -1.56 | 0.84 |
| SMRW | -15.27 | 0.02* |

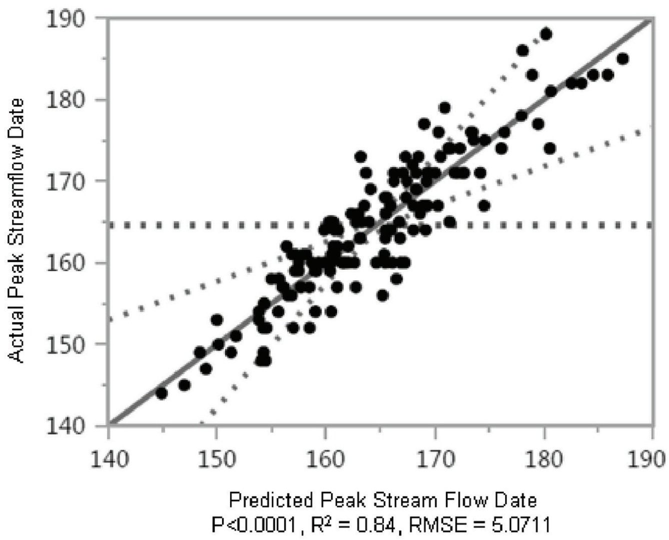


FIGURE 6. Peak streamflow model. GLS model fit for the date at which the average peak streamflow occurs (in number of days after 1 Jan), for all three watersheds. The mean of the response is demonstrated by the horizontal-dotted-line, and the limits of the 0.90 confidence intervals are represented by the diagonal-dotted-lines.

Table 7 shows that the most significant explanatory variables for determining the time of streamflow peaks are the average maximum February temperature and the average maximum and minimum May temperatures. The model suggests that with an average increase in maximum temperature of 1°C for February, peak streamflow shifts, on average, approximately one day later. Similar to the effect on the timing of the onset of the spring-pulse, a warmer average maximum February temperature prevents precipitation from falling as snow, resulting in less available snowpack pack for spring snowmelt. The average maximum and minimum May temperatures are also seen to affect the timing of peak streamflow. In general, an increase in average maximum and minimum temperatures causes streamflow to peak approximately two days sooner.

TABLE 8. GLS peak streamflow model site-specific estimates with corresponding p-values. Estimates in number of days, for all three watersheds (Levels of significance: * $\alpha = 0.05$; ** $\alpha = 0.01$).

| Site | Estimate | P- value |
|---|---|---|
| URW | 10.06 | 0.03* |
| ARW | -11.77 | 0.002** |
| SMRW | 1.714 | 0.57 |

Location has a significant effect on the timing of peak streamflow for the URW and the ARW (Table 8). Interestingly the shift in timing for the URW and the ARW was opposite. In comparison, the URW, on average experienced peak streamflow approximately ten days later than the average peak streamflow date, and the ARW experienced peak streamflow approximately twelve days earlier than the average peak streamflow date. These differences could possibly be the result of differing aspects.

GLS regression determined at a level of 0.99 significance, that the selected explanatory variables explained 82% of the variance associated with the date at when streamflow ended or substantially subsided (Fig. 7).

The date when streamflow ended, however, was affected by fewer explanatory variables when compared to the previous two models. The model for the end date suggests

that the explanatory variable with the highest confidence level is the average maximum November temperature (Table 9). More specifically, an average increase in maximum temperature of 1°C in November results in streamflow ending on average eleven days later.

Although site did not prove to be a statistically significant explanatory variable for predicting the end of streamflow, the relative magnitude of the estimates should still be taken into account. For instance, Table 10 shows that the for the URW and SMRW the timing of the end of streamflow is predicted to shift on average, approximately forty days earlier and forty

TABLE 7. GLS peak streamflow model. Individual explanatory variable estimates (in days) with corresponding p-values, for all three watersheds (Levels of significance: * $\alpha = 0.05$).

| Month | Average Tmax. | | Average Tmin. | | Average Precipitation | |
|---|---|---|---|---|---|---|
| | Estimate | P- value | Estimate | P- value | Estimate | P- value |
| January | 0.31 | 0.61 | 0.67 | 0.18 | 0.00 | 0.93 |
| February | 1.25 | 0.02* | -0.60 | 0.25 | 0.02 | 0.78 |
| March | -0.51 | 0.33 | 0.00 | 0.99 | -0.09 | 0.17 |
| April | -0.03 | 0.96 | 0.80 | 0.28 | 0.15 | 0.06 |
| May | -1.55 | 0.02* | -2.06 | 0.02* | 0.07 | 0.51 |
| June | -1.41 | 0.05 | -0.27 | 0.76 | 0.03 | 0.73 |
| July | 0.03 | 0.96 | 0.83 | 0.30 | 0.11 | 0.23 |
| August | 0.61 | 0.35 | 0.37 | 0.64 | 0.16 | 0.06 |

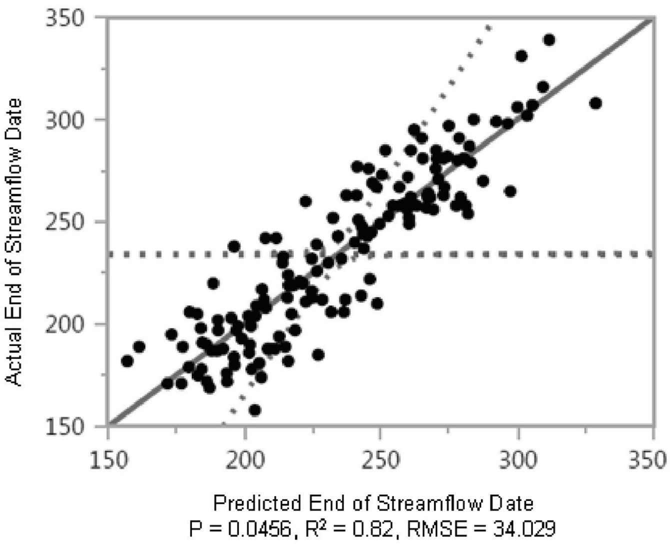


FIGURE 7. End of streamflow model. GLS model fit for the date at which streamflow ends (in number of days after 1 Jan), for all three watersheds. The mean of the response is demonstrated by the horizontal-dotted-line, and the limits of the 0.90 confidence intervals are represented by the diagonal-dotted-lines.

days later, respectively. In general, we suggest that the most substantial negative effects for the date at which streamflow subsides are associated with increases in the average maximum temperatures during winter and spring months. This is likely because warmer temperatures earlier in the year cause less snow accumulation and earlier snowmelt, so less water is available later in the year.

TABLE 10. GLS end of streamflow model site-specific estimates with corresponding p-values. Estimates in number of days for all three watersheds, individually.

| Site | Estimate | P-value |
|---|---|---|
| URW | -46.83 | 0.35 |
| ARW | 2.85 | 0.95 |
| SMRW | 43.98 | 0.20 |

## DISCUSSION AND CONCLUSION

Changes in the timing and accumulation of snowpack significantly affect the hydrology of the western United States. In many montane regions, variability in weather phenomena causes a reduction in snowpack and earlier spring runoff that results in changes in the timing and volume of snowmelt-dominated stream-flow. Shifts in the timing of streamflow have significant implications for water management.

Recent studies (Kunkel et al., 2007; Diaz and Bradley, 1997; Eischeid et al., 1995; Christensen, 2004) have shown that the mountain region of the interior southwestern United States has warmed at one of the highest rates in the continental U.S. for the first part of the 21st Century. It is logical to assume that such warming will affect the timing of montane streamflow. Unfortunately, the nature of such effects is not fully understood. Understanding the nature of a potentially shifting flow regime is crucial for the future of water resource management (Luce and Holden, 2009).

Time-series analysis and linear-regression models were developed to identify any potential trends in the timing and vol-

TABLE 9. GLS end of streamflow model. Individual explanatory variable estimates (in days) with corresponding p-values, for all three watersheds (Levels of significance: * α = 0.05).

| Month | Average Tmax. | | Average Tmin. | | Average Precipitation | |
|---|---|---|---|---|---|---|
| | Estimate | P- value | Estimate | P- value | Estimate | P- value |
| January | 3.65 | 0.49 | -3.22 | 0.44 | 1.18 | 0.26 |
| February | -5.9 | 0.29 | 6.55 | 0.15 | 0.00 | 0.99 |
| March | -6.1 | 0.25 | 0.30 | 0.95 | -1.26 | 0.06 |
| April | 5.89 | 0.38 | -5.29 | 0.48 | -0.17 | 0.84 |
| May | -7.03 | 0.28 | 0.79 | 0.93 | 0.09 | 0.93 |
| June | -1.18 | 0.84 | 1.42 | 0.86 | -0.23 | 0.83 |
| July | 1.57 | 0.81 | 10.6 | 0.21 | -0.19 | 0.82 |
| August | 2.73 | 0.69 | -12.22 | 0.15 | 1.25 | 0.17 |
| September | -8.73 | 0.09 | 7.75 | 0.30 | 1.07 | 0.09 |
| October | -1.75 | 0.60 | 6.76 | 0.22 | -0.20 | 0.72 |
| November | 10.56 | 0.04* | -10.63 | 0.08 | 0.84 | 0.36 |
| December | -9.52 | 0.05 | 4.15 | 0.47 | -0.77 | 0.36 |

ume of streamflow as well as the level of correlation between selected weather variables. As a result of the considerable inter-annual variability in the timing of streamflow, illustrated in Figures 2, 3, and 4, none of the observed trends in shifting flow regimes are significant at the 0.90 significance level. The nature of the observed trends, however, suggests that streamflow is beginning earlier, peaking earlier and in some cases, possibly lasting longer into the year. In comparing the observed trends at each location, it is likely that site specific relationships exist between weather phenomena and flow regimes.

Multiple highly significant correlations occur between specific weather phenomena and the timing of streamflow, which resulted in positive and negative trends. Our general findings suggest that the timing of montane streamflow regimes can be sufficiently explained by average monthly maximum and minimum temperatures and average monthly precipitation. GLS regression determined, at a level of 0.99 significance, that the selected explanatory variables explained 56% of the variance associated with the date at which the onset of the spring-pulse occurs, 84% of the variance associated with the timing of peak streamflow, and 82% of the variance associated with the date at which streamflow ends, or substantially subsides.

In general, increases in average maximum temperatures for winter months have the most substantial effect in terms of shifting the onset of the spring-pulse later and increases in average minimum temperatures for spring months have the most substantial effect in terms of shifting the onset of the spring-pulse earlier. This change is likely because an increase in average winter maximum temperatures prevents precipitation from falling as snow, resulting in less available snowpack pack come time for spring snowmelt. Conversely, an increase in average minimum temperatures for spring months results in earlier spring snowmelt.

Earlier snowmelt and streamflow are likely to become an increasingly challenging problem for many water resource management systems. With changing weather phenomena, snowmelt dominated streams are becoming less predictable and less reliable (Dettinger and Cayan, 1995; Dettinger and Diaz, 2000). Although the complex nature of montane hydrologic systems is not fully understood, the ability to characterize which basins that are impacted by specific weather phenomena is a crucial step towards understanding future changes and water resource vulnerability.

## ACKNOWLEDGMENTS

We thank Dr. Hongbin Zhan (Endowed Ray C. Fish Professor, Texas A&M University) and Dr. Kevin R. Gamache for their resourceful inputs and comments on the manuscript.

## REFERENCES

Barker, T., Bashmakov, I., Bernstein, L., Bogner, J., Bosch, P., Dave, R., Davidson, O., Fisher, B., Grubb, M., Gupta, S., Halsnaes, K., Heij, B., Kahn Ribeiro, S., Kobayashi, S., Levine, M., Martino, D., Masera Cerutti, O., Metz, B., Meyer, L., Nabuurs, G., Najam, A., Nakicenovic, N., Rogner, H., Roy, J., Sathaye, J., Schock, R., Shukla, P., Sims, R., Smith, P., Swart, R., Tirpark, D., Urge-Vorsatz, D., Zhou, D., 2007, Climate change 2007: Synthesis report: Washington D.C. Intergovernmental Panel on Climate Change, p. 1-52.

Christensen, N.S., 2004, The effects of climate change on the hydrology and water resources of the Colorado River basin: Climatic Change, v. 62, p. 337-363.

Dettinger, M.D., and Cayan, D.R., 1995, Large-scale atmospheric forcing of recent trends toward early snowmelt runoff in California: Journal of Climate, v. 8, p. 606-623.

Dettinger, M.D., and Diaz, H.F., 2000, Global characteristics of stream flow seasonality and variability: Journal of Hydrometeorology, v. 1, p. 289-310.

Diaz, H.F., and Bradley, R.S., 1997, Temperature variations during the last century at high elevation sites: Climatic Change at High Elevation Sites: Climatic Change, v. 36, p. 253-279.

Eischeid, J.K., Baker, C.B., Karl, T.R., Diaz, H.F., 1995, The quality control of long-term climatological data using objective data analysis: Journal of Applied Meteorology, v. 34, p. 2787-2795.

Ficklin, D.L., Stewart, I.T., Maurer, E.P., 2013, Climate change impacts on streamflow and subbasin-scale hydrology in the upper Colorado River basin: PloS One, v. 8, e71297.

Inyan, B.J., and Williams, M.W., 2001, Protection of headwater catchments from future degradation: San Miguel River Basin, Colorado: Mountain Research and Development, v. 21, p. 54-60.

Jasper, K., 2004, Differential impacts of climate change on the hydrology of two alpine river basins: Climate Research, v. 26, p. 113-129.

Kunkel, K.E., Palecki, M.A., Hubbard, K.G., Robinson, D.A., Redmond, K.T., and Easterling, D.R., 2007, Trend identification in twentieth-century US snowfall: The challenges: Journal of Atmospheric & Oceanic Technology, v. 24, p. 64-73.

Luce, C.H., and Holden, Z.A., 2009, Declining annual streamflow distributions in the Pacific Northwest United States, 1948–2006: Geophysical Research Letters, v. 36, p. 1-6.

McCabe, G. J., and Clark, M.P., 2005, Trends and variability in snowmelt runoff in the western United States: Journal of Hydrometeorology, v. 6, p. 476-482.

McCabe, G. J., and Wolock, D.M., 2007, Warming may create substantial water supply shortages in the Colorado River basin: Geophysical Research Letters, v. 34, p. 1-5.

Nolin, A.W., 2012, Perspectives on climate change, mountain hydrology, and water resources in the Oregon Cascades, USA: Mountain Research and Development, v. 32, p. 35-46.

Nydick, K., Crawford, J., Bidwell, M., Livensperger, C., Rangwala, I., Cozetto, K., 2012, Climate Change Assessment for the San Juan Mountain Regions, Southwestern Colorado, USA: A Review of Scientific Research: Durango, Mountain Studies Institute, USDA San Juan National Forest Service, USDOI Bureau of Land Management, p. 1-112 (static1.squarespace.com/static/53bc5871e4b095b6a42949b4/t/551997a5e4b0c6d76aa21bbd/1427740581512/ClimateResearchReview_SJMs_FINAL.pdf).

Rangwala, I., and Miller, J.R., 2010, Twentieth century temperature trends in Colorado's San Juan Mountains: Arctic, Antarctic, and Alpine Research, v. 42, p. 89-97.

Ray, A.J., Barsugli, J.J., Averyt, K.B., Wolter, K., Hoerling, M., Doesken, N., Udall, B., and Webb, R.S., 2008, Climate change in Colorado: A synthesis to support water resources management and adaptation: Boulder, Intermountain West Climate Summary, University of Colorado, p. 2-4 (wwa.colorado.edu/climate/iwcs/archive/IWCS_2008_Nov_feature.pdf).

Regonda, S.K., Rajagopalan, B., Clark, M., Pitlick, J., 2005, Seasonal cycle shifts in hydroclimatology over the western United States: Journal of Climate, v. 18, p. 372-384.

Slack, J.R., and Landwehr, J.M., 1994, Hydro-climatic data network (HCDN): A US Geological Survey streamflow data set for the United States for the study of climate variations, 1874-1988: US Geological Survey, Open-File Report, p. 92-129.

Stewart, I. T., Cayan, D.R., and Dettinger, M., 2004, Changes in snowmelt runoff timing in western North America under abusiness as usual climate change scenario: Climatic Change, v. 62, p. 217-232.

Tague, C., Grant, G., Farrell, M., Choate, J., Jefferson, A., 2008, Deep groundwater mediates streamflow response to climate warming in the Oregon Cascades: Climatic Change, v. 86, p. 189-210.

Tague, C., and Grant G.E., 2009, Groundwater dynamics mediate low-flow response to global warming in snow-dominated alpine regions: Water Resources Research, v. 45, p. 225-276.

Timilsena, J., Piechota, T., Tootle, G., Singh, A., 2009, Associations of inter-decadal/interannual climate variability and long-term Colorado River basin streamflow: Journal of Hydrology, v. 365, p. 289-301.

Toney, J.L, and Anderson, R.S., 2006, A post-glacial palaeoecological record from the San Juan Mountains of Colorado, USA: fire, climate and vegetation history: The Holocene, v. 16, p. 505–517.

Uncompahgre Watershed Partnership, 2013, Uncompahgre Watershed Plan: www.uncompahgrewatershed.org.

Uhlenbrook, S., Didszun, J., and Leibundgut, C., 2005, Runoff generation processes on hillslopes and their susceptibility to global change: Global Change and Mountain Regions, v. 23, p. 297-207.

Viviroli, D., Archer, D.R., Buytaert, W., Fowler, H.J., Greenwood, G., Hamlet, A.F., and Lorentz, S., 2011, Climate change and mountain water resources: overview and recommendations for research, management and policy: Hydrology and Earth System Sciences, v. 15, p. 471-504.

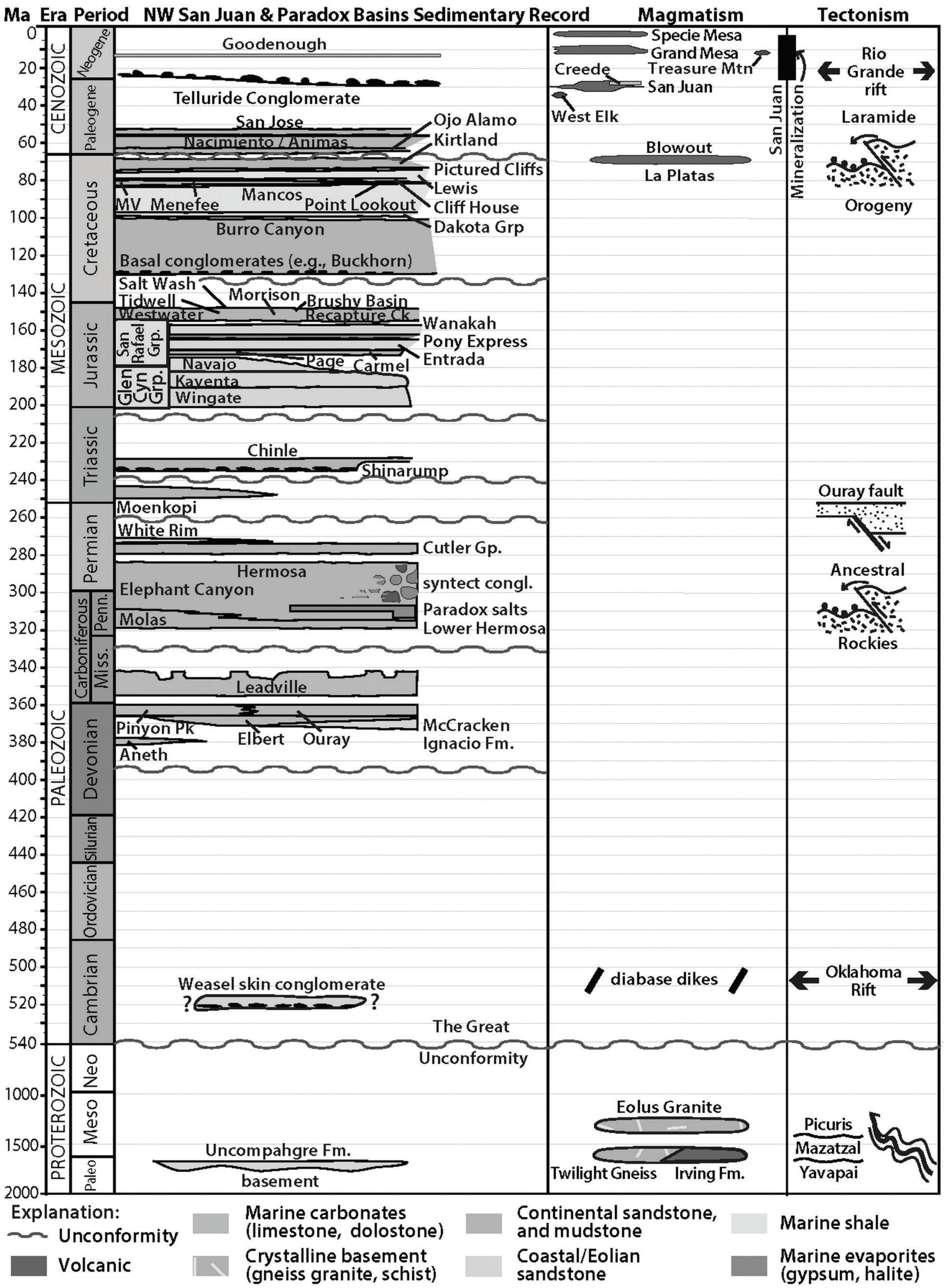

Ma Era Period NW San Juan & Paradox Basins Sedimentary Record Magmatism Tectonism
CENOZOIC
MESOZOIC
PALEOZOIC
PROTEROZOIC
Neogene
Paleogene
Cretaceous
Jurassic
Triassic
Permian
Carboniferous
Penn.
Miss.
Devonian
Silurian
Ordovician
Cambrian
Neo
Meso
Paleo
Goodenough
Telluride Conglomerate
San Jose
Nacimiento / Animas
Ojo Alamo
Kirtland
Pictured Cliffs
Lewis
Cliff House
Dakota Grp
MV Menefee
Mancos
Point Lookout
Burro Canyon
Basal conglomerates (e.g., Buckhorn)
Salt Wash
Tidwell
Westwater
Morrison
Brushy Basin
Recapture Ck
Wanakah
Pony Express
Entrada
San Rafael Grp.
Glen Cyn Grp.
Navajo
Page
Carmel
Kayenta
Wingate
Chinle
Shinarump
Moenkopi
White Rim
Cutler Gp.
Hermosa
Elephant Canyon
syntect congl.
Paradox salts
Lower Hermosa
Molas
Leadville
Pinyon Pk
Elbert
Ouray
McCracken
Ignacio Fm.
Aneth
Weasel skin conglomerate
The Great
Unconformity
Uncompahgre Fm.
basement
Specie Mesa
Grand Mesa
Creede
Treasure Mtn
San Juan
West Elk
Blowout
La Platas
diabase dikes
Eolus Granite
Twilight Gneiss
Irving Fm.
San Juan Mineralization
Rio Grande rift
Laramide
Orogeny
Ouray fault
Ancestral
Rockies
Oklahoma Rift
Picuris
Mazatzal
Yavapai
Explanation:
Unconformity
Volcanic
Marine carbonates (limestone, dolostone)
Crystalline basement (gneiss granite, schist)
Continental sandstone, and mudstone
Coastal/Eolian sandstone
Marine shale
Marine evaporites (gypsum, halite)